Chinese Herbal Medicines 16 (2024) 599–611

Contents lists available at ScienceDirect

Chinese Herbal Medicines

journal homepage: www.elsevier.com/locate/chmed

Original Article

Metabolomics combined with network pharmacology reveals anti-asthmatic effects of *Nepeta bracteata* on allergic asthma rats

Kailibinuer Abulaiti [a], Miheleayi Aikepa [a], Mireguli Ainaidu [a], Jiaxin Wang [a], Maiwulanijiang Yizibula [b], Maihesumu Aikemu [a,*]

[a] *Institute of Traditional Uyghur Medicine, Xinjiang Medical University, Urumqi 830017, China*
[b] *Central Laboratory Institute, Xinjiang Medical University, Urumqi 830011, China*

ARTICLE INFO

Article history:
Received 28 August 2023
Revised 15 November 2023
Accepted 16 February 2024
Available online 26 March 2024

Keywords:
allergic asthma
MAPK
metabolomics
network pharmacology
Nepeta bracteata Benth.
NOS2
STAT3

ABSTRACT

Objective: To investigate the mechanisms that underlie the anti-asthmatic effects of *Nepeta bracteata* (DBJJ, Dabao Jingjie in Chinese) in rats by integrating metabolomics and network pharmacology.
Methods: In this study, the rat model of asthma was induced by ovalbumin (OVA), and the rats were treated with a decoction of *N. bracteata*. Pathological changes in lung tissue were observed, and the quantification of eosinophils (EOS) and white blood cells (WBC) in bronchoalveolar lavage fluid was performed. Furthermore, the serum levels of asthma-related factors induced by OVA were assessed. ^{1}H NMR spectroscopy serum metabolomics method was utilized to identify differential metabolites and their associated metabolic pathways. UPLC-QE-MS/MS combined with network pharmacology was employed to predict the core targets and pathways of DBJJ in its action against asthma. The anti-asthmatic properties of DBJJ were investigated using an integrated approach of metabolomics and network pharmacology. The findings were validated through molecular docking and Western blotting analysis of the key targets.
Results: The administration of DBJJ effectively alleviated OVA-induced lung histopathological changes and decreased the number of EOS and WBC in BALF. Additionally, DBJJ inhibited the OVA-induced elevation of TNF-α, IL-18, Ig-E, EOS, IL-1β, MDA, VEGF-A, and TGF-β1. A total of 21 biomarkers and 10 pathways were found by metabolomics analysis. A total of 29 compounds were identified by UPLC-QE-MS/MS, in which 13 active components were screened by oral availability and Caco-2 cell permeability, the 120 targets and 173 KEGG pathways were predicted. The integration of metabolomics and network pharmacological analysis revealed that DBJJ's main constituents, including ferulic acid and ursolic acid, exerted their effects on four targets, namely DAO and NOS2, as well as their associated metabolites and pathways. The active constituents of DBJJ demonstrated a high binding affinity towards DAO and NOS2. Furthermore, DBJJ was observed to decrease the protein expression and phosphorylation levels of NOS2, MAPK, and STAT3.
Conclusion: The administration of DBJJ demonstrates notable anti-asthma properties in rats with allergic asthma. This effect can be attributed to the modulation of various targets, including NOS2, MAPK, and STAT3, by primary constituents such as ferulic acid and ursolic acid.

1. Introduction

Asthma is a prevalent chronic respiratory disease, and according to data from the World Health Organization (WHO), approximately 339 million people worldwide were affected by asthma in 2021. Children are disproportionately impacted by this condition (2022 Gina Main Report). With the continuous increase in human activities and environmental pollution, the incidence of asthma is steadily rising each year. This trend has significant implications for public health (Cevhertas et al., 2020). The etiology of asthma still remains elusive. However, current research suggests that airway hyperresponsiveness (AHR) is a prominent characteristic of asthma. AHR serves as a direct indicator of the severity of the condition. Airway inflammation is a ubiquitous pathological feature found in all subtypes of asthma and represents a central aspect of the disease. Furthermore, airway remodeling is a significant

* Corresponding author.
E-mail address: 1366102645@qq.com (M. Aikemu).

https://doi.org/10.1016/j.chmed.2024.02.001
1674-6384/

pathological feature that is closely associated with airway inflammation, immune imbalance, oxidative stress, AHR, and other contributing factors (Cevhertas et al., 2020; Wu, Brigham, & McCormack, 2019; Borna et al., 2019).

Currently, the treatment of asthma worldwide primarily involves the use of β2-receptor agonists, theophylline, anticholinergic drugs, glucocorticoids, non-steroidal anti-inflammatory drugs, mast cell membrane stabilizers, and leukotriene regulators (Charles et al., 2022; Ducharme, Tse, & Chauhan, 2014). However, despite their widespread use, these pharmacological agents exhibit limited efficacy and fail to comprehensively address the full range of asthma symptoms. Therefore, it is necessary to identify effective therapeutic drugs to treat this refractory disease (Cloutier et al., 2020).

Nepeta bracteata Benth. (DBJJ, Dabao Jingjie in Chinese), also known as "zufa", is a medicinal herb used in traditional Uyghur medicine and folk medicine. Its water decoction is traditionally used for relieving asthma, dissipating phlegm, and benefiting the lungs (Wang et al., 2016; Yang et al., 2022). Flavonoids have anti-inflammatory and anti-allergic effects, which can provide relief in conditions like asthma and allergies (Maleki, Crespo, & Cabanillas, 2019). They may also support immune function and have antimicrobial properties. It is reported that DBJJ contains flavonoids such as rutin, quercetin, luteolin and apigenin (Dolkun, Abduwak, Jinfang, Ye, & Anwar, 2022). Our previous research revealed that the total flavonoids of DBJJ possess anti-inflammatory, antitussive, expectorant, and anti-asthmatic effects (Yusupu & Aikemu, 2016). It has been found that the total polysaccharides from extract of DBJJ can significantly reduce the levels of IL-4, IL- 6, and IL-17 in the serum of asthmatic rats. This finding demonstrates the ability of DBJJ to alleviate the inflammatory response associated with asthma (Yang et al., 2022). It was discovered that the extract of DBJJ could effectively reduce the levels of serum TGF-β and Smad2/3 protein in asthmatic mice (Wang et al., 2016). Another study reported that DBJJ has the ability to improve airway inflammation in asthmatic rats, reduce AHR in a mouse model of bronchial asthma, and regulate the balance of Th17/Treg cell differentiation. However, the compound basis and the underlying mechanism of action of DBJJ in its antiasthma effects are still not fully understood, as reported by Zhang et al (2021).

Metabolomics is a systematic approach used to monitor the dynamic changes in small-molecule metabolites within living organisms. In recent years, scholars have increasingly utilized various technologies, such as network data mining, molecular docking, and integration with data from metabolomics experiments, to analyze the metabolic pathways and targets of traditional Chinese medicines (Zhang et al., 2021). Docking is a computational method used in the field of structural biology to predict and analyze the interactions between small molecules, such as drugs or ligands, and target biomolecules, such as proteins or nucleic acids. It plays a crucial role in drug discovery and design, as it helps scientists understand how a drug molecule binds to its target and enables the identification of potential high-affinity compounds. This integrated approach aims to enhance the accuracy of conclusions drawn from these studies (Liu, Mao, Gu, He, & Hu, 2021; Niu & Miao, 2022; Sun & Zhang, 2018; Zhang & Yi, 2020).

In this study, a rat model of allergic asthma was established using ovalbumin (OVA), followed by the administration of a DBJJ decoction as a treatment, and serum and bronchoalveolar lavage fluid (BALF) were used to evaluate the curative effect. The mechanism of DBJJ in the treatment asthma was explored by metabolomics combined with network pharmacology and verified by Western blotting analysis, and a more reliable conclusion was obtained.

2. Materials and methods

2.1. Reagents and materials

DBJJ was obtained from the Second People's Hospital of Xinjiang Uygur Autonomous Region and was identified by an associate researcher, Amatijiang, at the Institute of Drug Inspection and Research, Xinjiang Uygur Autonomous Region, as *Nepeta bracteate* Benth. It belongs to the Labiatae family and is obtained in the form of dried whole grass and stored at Xinjiang Uygur Autonomous Region Drug Testing and Research Institute, Department of Scientific Research and Technology with specimen No. 21102102.

OVA (A5503) and aluminum hydroxide dry powder (A5506) were obtained from Sigma (Milwaukee, USA). Dexamethasone (D8040) was purchased from Solarbio (Beijing, China). Rat IL-1β, eosinophils (EOS), white blood cells (WBC), malondialdehyde (MAD), superoxide dismutase (SOD), vascular endothelial growth factor-A (VEGF-A), tumor necrosis factor-alpha (TNF-α), immunoglobulin E (Ig-E), IL-18, and transforming growth factor-beta 1 (TGF-β1) enzyme-linked immunosorbent assay (ELISA) kits were obtained from Elabscience Biotechnology Co., Ltd. (Wuhan, China). D2O (Sigma-Aldrich, Lot No. MKBG0206V), TSP (CIL, Lot No. 1–17273), K_2HPO_4-$3H_2O$ (Sinopharm Chemical Reagent Co., Lot No. 20210629), NaH_2PO_4-$2H_2O$ (Sinopharm Chemical Reagent Co., Lot No. 20210209); Inova 600 NMR spectrometer, Varian, USA. Electrophoresis instrument (Beijing June 1 Instrument Factory DYY-7C, Beijing, China). Vertical electrophoresis cell, electrophoresis instrument and electric rotating instrument were obtained from Beijing Liuyi Biotechnology Co., Ltd. (Beijing, China), Enzyme-labeled Instrument was obtained from Thermo (Waltham, Massachusetts, USA), model devices of centrifuge was obtained from Hunan Xiangyi Laboratory Instrument Development Co., Ltd. (HI650, Changsha, China).

Enzyme labeling instrument (Thermo mμlISKANMK3, Waltham, Massachusetts, USA), RIPA Lysis Buffer (Biyotime P0013B), BCA protein concentration determination kit (Beyotime P0010), INOS, MAPK1, MAPK3, STAT3 were obtained from Affinity Biosciences (Liyang, China).

2.2. DBJJ decoction

To prepare DBJJ decoction, 50 g of the substance was weighed and placed in a 3 000 mL capacity frying pan. Subsequently, 2 500 mL of water was added to the pan, and the mixture was simmered for 1 h. After simmering, the mixture was filtered while still hot, and the filter residue was further treated by adding 2 000 mL of water. The mixture was simmered for an additional hour and filtered again while still hot. The two filtrates were combined, and the resulting mixture was heated over medium heat until it was condensed to a final volume of 100 mL.

2.3. Preparations of animals and feeding

The 50 SD rats, weighing (200 ± 20) g, both male and female, were obtained from the Animal Experiment Center of Xinjiang Medical University North Campus. The rats belonged to the SPF class and were provided under license number: SYXK (new) 2018-0003. All experimental procedures were conducted in strict compliance with the relevant provisions of the "Regulations on the Management of Laboratory Animals" issued by the State Science and Technology Commission. The animals were housed in a sterile environment within a laboratory that met SPF class standards. The temperature in the environment was maintained at (20 ± 3) °C, with a humidity level of (40 ± 5)%. The rats were randomly divided into five groups: control group (Control), asthma

group (Model), high-dose DBJJ group (DBJJ-HG), low-dose DBJJ group (DBJJ-LG), and dexamethasone (DXMS) group.

The experimental protocol was approved by the Animal Ethics Committee of the Institutional Animal Care and Use Committee of Xinjiang Medical University, with an approval number of IACUC-20210305–06. The animal experiment was conducted in accordance with the guidelines outlined in the 2017 Chinese Experimental Animal Management Law. Throughout the experimental period, the rats were provided with normal food and water ad libitum.

2.4. Replication of asthma rat model and treatment protocols

Asthma was induced in the rats by intraperitoneal injection of Al $(OH)_3$ (100 mg) and OVA at a dose of 1 mg/kg to sensitize them. After a period of 14 d, the rats were placed in a closed box and exposed to 1 % OVA aerosol through airflow for 20 min per day over a span of 14 d (Kianmeher, Ghorani, & Boskabady, 2016). The rats were then divided into four groups: normal control group, asthma group, and sensitized with OVA but treated with normal saline (model); DBJJ-HG group treated with a dose of 0.4 g/kg of DBJJ; DBJJ-LG group treated with a dose of 0.2 g/kg of DBJJ; DXMS group given dexamethasone via oral gavage at a concentration of 0.125 g/kg.

2.5. Specimen collection

At the end of the experiment, the rats were fasted for 24 h with access to water. They were then anesthetized by intraabdominal injection of pentobarbital sodium at a dose of 50 mg/kg. Lung tissue, abdominal aortic blood, and BALF were collected. The collected blood was allowed to stand at room temperature for 1 h and then centrifuged at 4 000 r/min for 15 min at 4 °C to obtain the serum. The serum samples were stored at −80 °C for subsequent metabolomic analysis and enzyme-linked immunosorbent assay (ELISA) testing. The collected BALF was also allowed to stand at room temperature for 1 h and then centrifuged at 12 000 r/min for 10 min at 4 °C. The supernatants were then removed for further analysis.

The lung was promptly dissected, and a scalpel blade was used to extract the lower lobe of the lung. The lower lobe was then placed in an embedding cassette for further processing. The superior lobe of the lung was placed in a 5 mL Eppendorf tube and stored at −80 °C for Western blotting analysis.

2.6. Histopathology

After undergoing dehydration, cleaning, and embedding in paraffin blocks, the preserved rat lung tissue in 10 % formalin was sliced into 5 μm thick sections using a microtome. These sections were subjected to deparaffinization in xylene, followed by rehydration using a series of graded ethanol solutions. Subsequently, the sections were stained with hematoxylin for 5 min, rinsed with tap water, and then stained with eosin for 2 min. After cleaning in xylene and dehydration in ethanol solutions, the sections were mounted on coverslips and examined under a light microscope at the appropriate magnification to gather relevant pathological data.

2.7. BALF cell counts and serum ELISA analysis

The number of EOS and WBC in BALF was quantified using a hemocytometer. Serum levels of TNF-α, IL-18, Ig-E, IL-1β, VEGF-A, TGF-β1, SOD, and MDA were determined using ELISA, following the manufacturer's instructions.

2.8. ^{1}H NMR serum metabolomics

To remove precipitates, 200 μL of serum was mixed with 400 μL of 0.2 mol/L phosphate buffer (0.2 mol/L K_2HPO_4/ NaH_2PO_4). For NMR spectroscopy, the supernatant was transferred to a 5 mm NMR tube with 100 L D2O. The plasma ^{1}H NMR spectra for each sample were obtained using an NMR spectrometer (Inova-600, Varian, USA) equipped with a 5 mm ID/PFG probe and operating at a proton frequency of 600 MHz. The Carr-Purcell-Meboom-Gill (CPMG) pulse sequence was used to obtain these spectra, and 64 scans were collected for each sample over a 10 000 Hz spectral width, resulting in an acquisition time of 1.64 s and a relaxation delay of 2 s at 32 K. The spectra were divided, and the signal integral was calculated at intervals of 0.003 ppm between 0.5 and 9.0 ppm after eliminating the spectral area between 4.70 ppm and 5.0 ppm. The normalized data were analyzed using SIMCA-P version 14.1 software (Umetrics, Umea, Sweden) for multivariate data analysis. Partial Least Squares Discriminant Analysis (PLS-DA) was used to validate the model, and Orthogonal Partial Least Squares Discriminant Analysis) (OPLS-DA) was used to optimize sample separation. The R^2Y and Q^2 values were used to assess the quality of the OPLS-DA model, which represents the explained model's analytic capability and predictability. To verify the accuracy of the OPLS-DA model, 200 permutations were run. Metabolites with $P < 0.05$ among different groups were selected as differentially expressed metabolites. The differential metabolites from ^{1}H NMR were uploaded to the MetaboAnalyst version 5.0 Pathway analysis database to investigate significantly distinct metabolic pathways.

2.9. UPLC-QE-MS/MS based untargeted compound analysis

The samples were thawed on ice, vortexed for 30 s, and then centrifuged at 12 000 r/min [RCF = 13 800 (× g), R = 8.6 cm] for 15 min at 4 °C. After centrifugation, 300 μL of supernatant was transferred to a fresh tube, and 1 000 μL of extracted solution containing 10 μg/mL of internal standard was added. The samples were sonicated for 5 min in an ice-water bath and then placed at −40 °C for 1 h. Subsequently, the sample was centrifuged again at 12 000 rpm for 15 min at 4 °C. The supernatant was carefully filtered through a 0.22 μm microporous membrane, and 100 μL from each sample was pooled as QC samples. The samples were stored at −80 °C until UPLC-QE-MS/MS analysis. LC-MS/MS analysis was performed on a UPLC system (Vanquish, Thermo Fisher Scientific) with a Waters UPLC BEH C_{18} column (100 mm × 2.1 mm, 1.7 μm). The flow rate was set at 0.4 mL/min and the sample injection volume was set at 5 μL. The mobile phase consisted of 0.1% formic acid in water (A) and 0.1% formic acid in acetonitrile (B). The multi-step linear elution gradient program was as follows: 0−3.5 min, 95%−85% A; 3.5−6 min, 85%−70% A; 6−6.5 min, 70%−70% A; 6.5−12 min, 70%−30% A; 12−12.5 min, 30%−30% A;12.5−18 min, 30%−0 A; 18−25 min, 100% B; 25−26 min, 0−95% A; 26−30 min, 95%−95% A. An Orbitrap Explores 120 mass spectrometer coupled with Xcalibur software was used to obtain the MS and MS/MS data based on the IDA acquisition mode. During each acquisition cycle, the mass range was from 100 to 1 500, and the top four of every cycle were screened and the corresponding MS/MS data were further acquired. The sheath gas flow rate was 30 Arb, the Aux gas flow rate was 10 Arb, Ion Transfer Tube Temp was 350 °C, Vaporizer Temp was 350 °C, Full MS resolution was 60 000, MS/MS resolution was 15 000, Collision energy was 16/38/42 in NCE mode, and Spray Voltage was 5 500 V (positive) or −4 000 V (negative). The raw data were converted to the mzXML format using Proteo Wizard and processed with an in-house program developed using R and based on XCMS for peak detection, extraction, alignment, and integration. An in-house MS2 database (tradi-

tional Chinese medicine database of Shanghai Biotree Biomedical Technology Co., Ltd.) was applied to annotate the components. Afterwards, the HMDB and KEGG public databases (https://www.kegg.jp/) were searched for corresponding substances with empty MS2 score columns.

2.10. Network pharmacology

(1) The phrase "asthma" was used to search for potential targets in the three gene map databases Online Mendelian Inheritance in Man (OMIM), Therapeutic Target Database and GeneCards. (2) Collection of active components of DBJJ by CNKI, PubMed. (3) Oral availability (OB) $\geq$ 30% and (CaCO-2) $\geq$ 0.3 as conditions for screening active components of DBJJ through Traditional Chinese Medicine Systems Pharmacology (TCMSP, https://tcmspw.com/tcmsp.php) and admetSAdatabase as the screening conditions to screen the effective compounds of DBJJ. (4) The SMILES structure of effective compounds was found through PubChems database (https://pubchem.ncbi.nlm.nih.gov), and then introduced into the SWISS Target Prediction database (https://www.swisstargetprediction.ch) to obtain the predicted targets of the screened compounds, the species selected "homo sapiens", took probability > 0.1 as the screening condition, obtained the effective target, and imported them into the UniProt database (https://www.uniprot.org/) to standardize the genes and proteins names. (5) Combine asthma targets with DBJJ-related targets in Venny (htttps://bioinfogp.cnb.csic.es/tools/venny/). (6) The PPI analysis was carried out by submitting overlapping targets of DBJJ and asthma to the STRING database (https://string-db.org/) in order to identify the primary regulatory targets more precisely. Homosapiens was the only species allowed, and a minimum interaction score of 0.9 was necessary. As with the core genes, the independent target protein nodes were concealed. (7) Subsequently, the PPI results were imported into Cytoscape 3.7.2, to structure the protein–protein interaction (PPI) network. At the same time, the CytoHuba plugin in Cytoscape 3.7.2 was used to analyze the core target for MCC analysis, which was used to screen the top 10 targets with the highest score as hub targets. (8) Import the key genes to the Metascape database (https://metascape.org) for Kyoto Encyclopedia of Genes and Genomes (KEGG) pathway enrichment analyses. (9) Validate the hub gene which are more significantly associated with asthma by Western blotting analysis.

2.11. Integrated metabolomics and network pharmacological analysis

Overlapping pathways between metabolic pathways and network pathways were identified as potential pathways for DBJJ in treating asthma. The targets for these overlapping pathways were obtained using the KEGG database. The drug-active component-target interaction network of DBJJ was analyzed to search for corresponding data using these target proteins. Subsequently, the interaction network of DBJJ treatment for asthma, including active compounds, key targets, pathways, and biomarkers, was established. Finally, the key targets were validated through Molecular Docking and Western blotting analysis.

2.12. Molecular docking

The active compounds were chosen as ligands for molecular docking. The three-dimensional structures of these active ingredients were acquired from PubChem (https://www.ncbi.nlm.nih.gov/). The conformational structure of the target protein was searched by PDB database (https://www.rcsb.org) and screened. The protein structure was obtained through X-ray crystal diffraction. Proteins with crystal resolutions below 1.5 and carrying their own small molecular ligands were selected as screening conditions. Hydrogen atoms and water molecules were removed from the protein macromolecules (receptors) using Auto Tools, while the small molecules (ligands) of the compounds underwent pre-processing. The energy lattice was calculated using Auto Grid, and the active sites of proteins with small molecular ligands were defined based on the location of original ligand. Subsequently, Auto Dock Vina was employed to perform the docking between the receptors and ligands, and binding energy was calculated. The docking results with the highest scores were visualized using Discovery Studio 4.5 Client.

2.13. Western blotting

The lung tissue was lysed and placed for 30 min. After centrifugation at 12 000 r/min for 5 min, the culture fluid was collected. The culture fluid was then diluted 20 times, and a standard protein with concentrations of 1.0, 0.8, 0.6, 0.4, and 0.2 mg/mL was prepared. Incubation was performed for 15 min at 37 °C while avoiding light to prevent protein denaturation. Boiling water bath treatment was applied for 10 min. The protein samples were then subjected to electrophoresis under constant pressure at 180 V for 60 min, until the bromophenol blue dye reached the bottom of the gel. Protein expression levels were detected using antibodies against GAPDH (1:1 000), INOS (1:1 000), MAPK (1:1 000), and STAT3 (1:1 000) as controls. The target proteins were blocked with 5% skim milk for 2 h and then incubated with primary and secondary antibodies. The membrane was treated with an ECL reinforcing reagent, and the gray value of the target protein was analyzed using image analysis software Proplus.

2.14. Statistical analysis

The data were presented as mean ± standard deviation. Multiple group comparisons were performed using One-way ANOVA and Dunnett's T3 test (GraphPad Prism 9), with a significance level of $P < 0.05$.

3. Results

3.1. Effects of DBJJ on WBC and EOS counts in BALF

The levels of inflammatory cells in BALF, specifically EOS and WBC, were found to be elevated in the model group compared to the control group. However, in the treatment groups (DBJJ-HG, DBJJ-LG, and DXMS), the levels of inflammatory cells were significantly decreased compared to the model group. Furthermore, there was a dose-dependent relationship observed, indicating that the reduction in inflammatory cells corresponded to the dose of the treatment (Fig. 1).

3.2. Effects of DBJJ on pulmonary pathological damage

As shown in Fig. 2, the control group demonstrated a normal and intact lung tissue structure. However, the model group displayed notable infiltration of inflammatory cells surrounding the bronchi, narrowed airways, thickened bronchial airway walls, and deposition of collagen around the airways. The treatment groups, on the other hand, exhibited significant improvements in symptoms such as pulmonary inflammation and airway stenosis. These observations indicate that the treatments effectively alleviated the pathological changes associated with asthma in the experimental model.

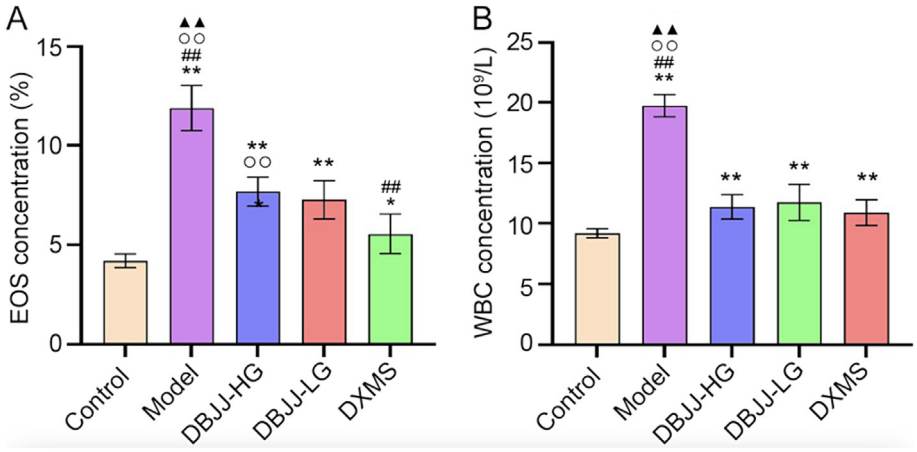

Fig. 1. Effects of DBJJ on inflammatory cell recruitment in BALF from asthmatic rats (mean ± SD, n = 10). Effects of DBJJ on percentage of EOS counts (A) and WBC counts (B) in asthmatic rats. $^{**}P < 0.01$ *vs* control group; $^{\#\#}P < 0.01$ *vs* DBJJ-HG group; $^{○○}P < 0.01$ *vs* DBJJ-LG group; $^{▲▲}P < 0.01$ *vs* DXMC group.

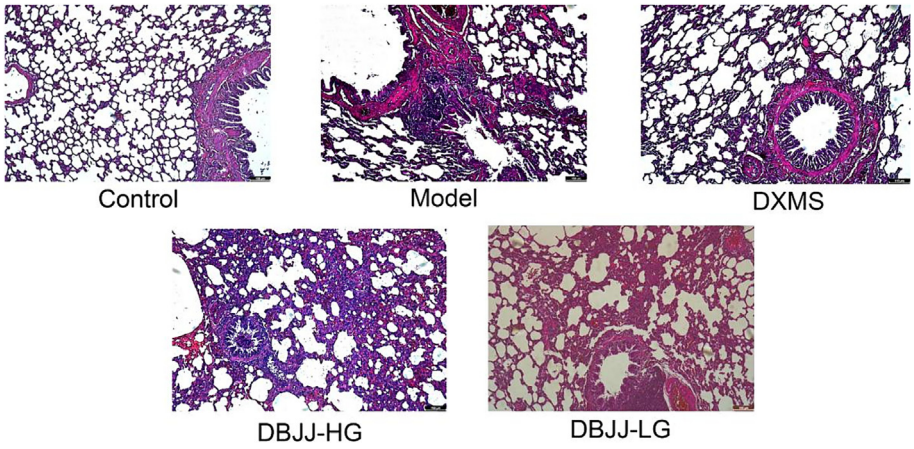

Fig. 2. Histological assessment of lung tissue. Representative micrographs of H&E staining of lung sections (×100).

3.3. Serum ELISA detection

The levels of TNF-α, IL-18, IgE, IL-1β, VEGF-A, TGF-β1, SOD were significantly increased in the model group, and MDA was significantly decreased compared with the control group ($P < 0.05$), while treatment with DBJJ resulted in significant decreases compared with the model group, and MDA was increased ($P < 0.05$) (Fig. 3).

3.4. ^{1}H NMR-based metabolic profiles in serum

The 30 metabolites (isoleucine, leucine, β-hydroxybutyric acid, lactic acid, alanine, glycoprotein glycine, tyrosine, phenylalanine, acetone, pyruvic acid, 1-methylhistidine, α-glucose, β-glucose, lipids (VLDL), methionine, creatine, citric acid, valine, 3-hydroxybutyrate, glutamic acid, glutamine, glutathione oxide, ethanolamine, succinic acid, aspartic acid, glycerophosphorylcholine, ethanolamine phosphate, betaine, hypoxanthine) of five groups were detected and identified by typical ^{1}H NMR spectra. The ^{1}H NMR serum spectra included small molecules from various metabolite classes, such as amino acids (e.g., tyrosine, glutamate and valine), TCA cycle intermediates (e.g., succinate), and carbohydrates (e.g., glucose). Representative 600 MHz ^{1}H NMR spectra obtain from serum samples of four groups was shown in Fig. S1.

3.5. Potential biomarkers and metabolic pathways

The integral values obtained from the segmented integration of the ^{1}H NMR spectrum were analyzed using principal component analysis (PCA) and PLS-DA methods. This analysis allowed us to generate 3D spatial maps and scatter plots of the rat serum ^{1}H NMR spectrum (Fig. 4A–C). The PCA-X score plots and OPLS-DA 3D score plots of the four groups clearly showed distinct differentiation. To ensure the reliability of the PLS-DA model, a 200-permutation test was performed. The outcome demonstrated the viability of model [R^2= (0.0, 0.038), Q^2= (0.0, −0.155)].

After applying a cutoff of $P < 0.05$ (using t-test), a total of 21 different metabolites, including isoleucine, β-hydroxybutyric acid, glycine, and succinic acid, were identified as significantly different between the DBJJ-HG group and model group (Table 1). These metabolites were considered potential biomarkers of DBJJ treatment for asthma.

3.6. Differential metabolite pathway analysis in serum

The above-mentioned differentiated metabolites were added to the MetaboAnalyst version 5.0 analysis database (https://www.metaboanalyst.ca). As prospective differential routes in this inves-

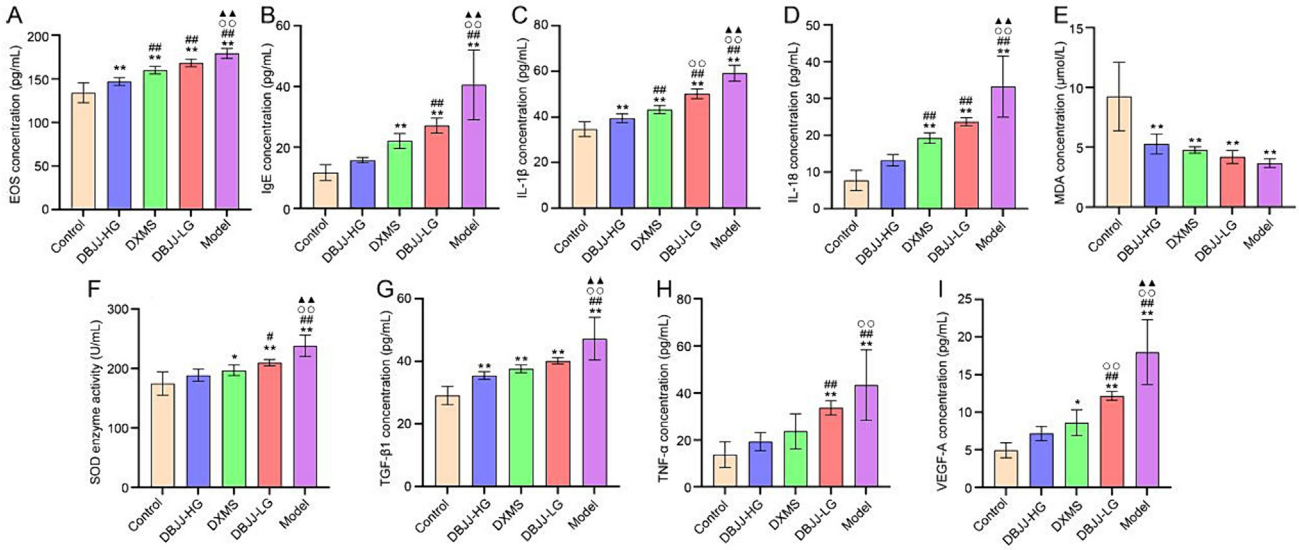

Fig. 3. Effects of DBJJ on serum indexes of EOS (A), IgE (B), IL-1β(C), IL-18(D), MDA (E), SOD (F), TGF-β1 (G), TNF-α (H), VEGF-A (I) from asthmatic rats (mean ± SD, n = 10). $^{*}P < 0.05$, $^{**}P < 0.01$ *vs* control group; $^{\#}P < 0.05$, $^{\#\#}P < 0.01$ *vs* DBJJ-HG group; $^{\bigcirc\bigcirc}P < 0.01$ *vs* DBJJ-LG group; $^{\blacktriangle\blacktriangle}P < 0.01$ *vs* DXMC group.

tigation, metabolic pathways with impact values greater than 0.10 were chosen. Finally, the relationship between metabolic pathways and metabolites was shown (Table 2 and Fig. 4D and E.).

3.7. UPLC-QE-MS/MS combined with network pharmacological analysis

3.7.1. Screening of active compounds and prediction of targets for DBJJ

Under the optimized analysis conditions, the total ion chromatograms of DBJJ in positive and negative ion modes were presented in Fig. 5. By conducting comparative analysis of MS and MS/MS mass spectrometry data, along with considering retention behavior and utilizing databases such as the Human Metabolome Database (HMDB) and relevant literature reports, a total of 29 components were successfully identified. The compounds identified in DBJJ can be classified into the following structural types: terpenoids (10), phenolic acids (4), flavonoids (7), phenylpropanoids (2), phenols (2), alkaloids (1), stilbenes (2), and phenylpropanoic acid (1). Additionally, considering the components reported in the literature that can be absorbed into the bloodstream and possess specific pharmacological activities, relevant active ingredients were included in the list of potential active compounds of DBJJ. As a result, a total of 13 active compounds were identified for DBJJ, as shown in Table 3.

3.7.2. Obtaining and analyzing targets of DBJJ for anti-asthma effects

Using the 13 active compounds identified, we obtained 281 targets through the TCMSP database (https://tcmspw.com/tcmsp.php). These targets were then used to construct a herb-active component-target interaction network for DBJJ (Fig. 6A). Additionally, we collected 5 987 asthma-related primary targets from various databases. By comparing these asthma targets with the active component targets of DBJJ, we identified 160 common targets that could potentially be targeted by DBJJ for the treatment of asthma (Fig. 6B), the target names were converted into gene symbols using the UniProt database. A PPI network was constructed using the String database and Cytoscape to screen the 120 core targets of DBJJ for the treatment of asthma, and MAPK1, STAT3, PTPN11, LCK, RXRA, HDAC1, RXRB, RXRG, RARA, FYN were selected as hub targets (Fig. 6C and D). KEGG enrichment analysis and GO enrichment analysis were performed on the core targets to assess their potential in alleviating asthma symptoms (Fig. 6E and F). The KEGG enrichment analysis identified 173 significantly affected pathways. From these pathways, we selected the top 20 pathways based on the corrected P value and visualized them in the form of bubble diagrams (Table 4), and based on the corrected P value to create bubble diagrams. It mainly involves such as the pathway of cancer, the application of AGE-RAGE signal pathway in diabetic complications, Th17 cell differentiation, proteoglycan in cancer, MAPK signal transduction pathway, endocrine resistance, regulation of TRP channel by inflammatory mediators, chemical carcinogenesis-reactive oxygen species (Ros), fluid shear stress and atherosclerosis, sphingomyelin signal transduction pathway, lipid and atherosclerosis, relaxer signal pathway, C lectin receptor signal transduction pathway, epidermis growth factor receptor tyrosine kinase inhibitor resistance, bladder cancer, chemical carcinogenic receptor activation, PI3K-Akt signal transduction pathway, and other metabolic pathways.

3.8. Integrated metabolomics and network pharmacology

By comparing 14 metabolic pathways and 173 KEGG network pathways, we identified two overlapping pathways: arginine and proline metabolism and glutathione metabolism. These pathways were considered potential treatment routes for asthma using DBJJ, as they serve as connections between metabolomics and network pharmacology. These pathways are responsible for the production of linked targets, active substances, herbs, and associated biomarkers. We constructed a network that includes four active compounds, four key targets, two pathways, and six biomarkers (Fig. 7A). This network provides a pharmacological perspective on how DBJJ may impact asthma.

3.9. Molecular docking

The active components of DBJJ were individually linked to the key targets, which were obtained from the previous analysis, through molecular docking. This allowed us to verify the binding strength between the active components and key targets. The binding affinity between the ligands (active components) and the

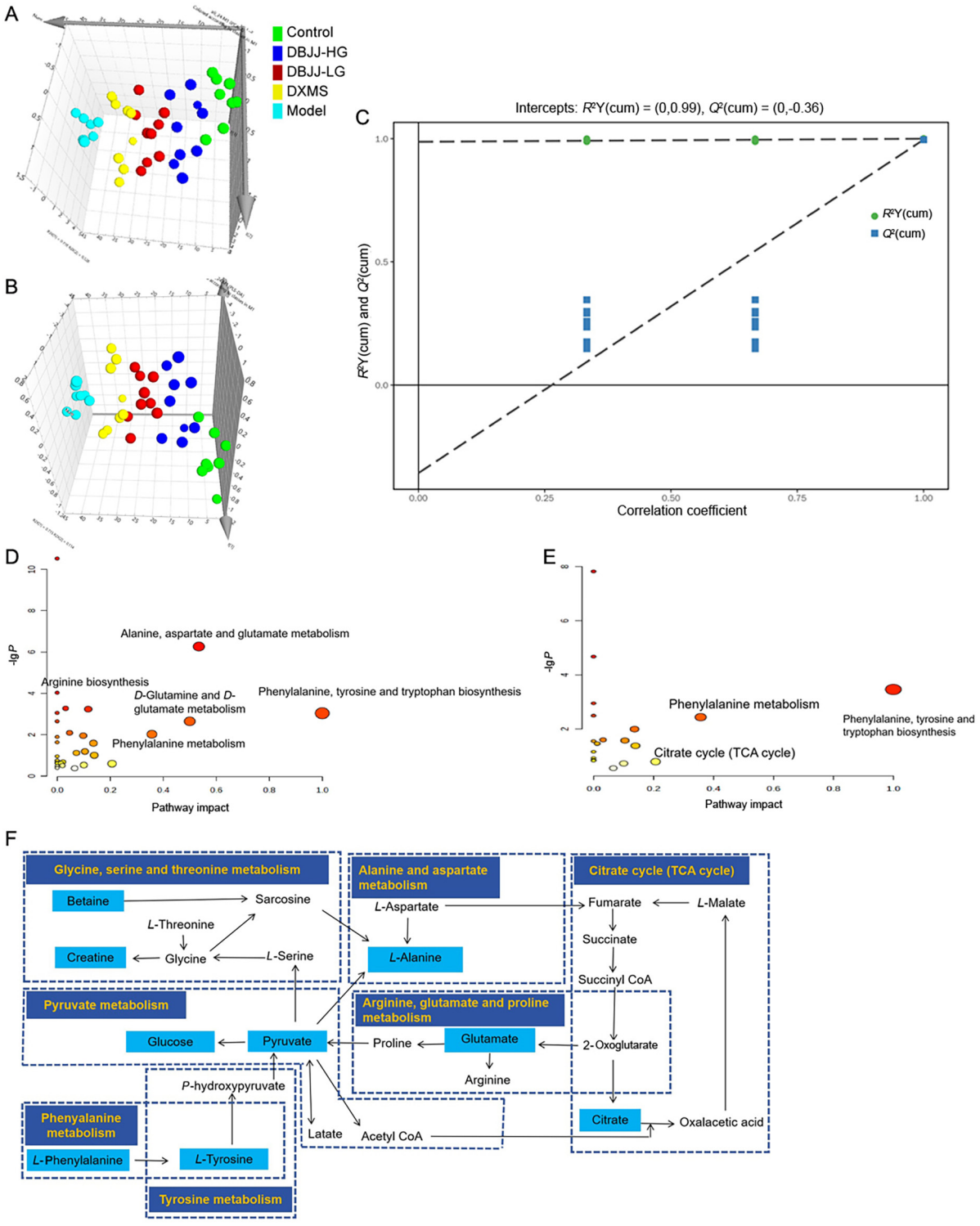

Fig. 4. Multivariate analysis based on serum metabolic profiles of four groups (n = 10). (A) PCA-X score plot for five groups (R2X:0.85; Q2:0.77); (B) PLS-DA 3D score plot for four groups; (C) Permutation test of PLS-DA for five groups (R2X:0.832; R2Y:0.215; Q2:0.118); Bubble plots of metabolic pathways analysis changed by DBJJ-HG *vs* model and changed by DBJJ-LG *vs* model (D, E). The altered metabolic pathways were represented as dots. The impact value at x-coordinate represents importance index of metabolic pathways obtained by topological analysis and calculation, and $-\lg P$ at y-coordinate represents significance level of enrichment analysis of metabolic pathways, the more compounds in pathway, the redder of color; (F) Schematic diagram of relationship between metabolic pathways and metabolites identified by analysis of rat ^{1}H NMR serum samples.

receptors (target proteins) was indicated by the connection score. A lower score value indicates better binding activity and stability. A score value of ≤ -7.00 suggests a strong and stable binding between the components and targets. The analysis revealed that the active components of DBJJ exhibited strong binding activity with the target proteins, as shown in Table 4 and Fig. 7B.

Table 1
Differentially expressed metabolites DBJJ *vs* model group (Fold change).

Metabolites	Chemical shift (p.m.)	DBJJ-HG *vs* Model	
		FC	*P* (corr)
Isoleucine	0.93(t), 1.00(d)	0.901	−0.827
Leucine	0.95(d), 0.97(d)	0.901	−0.754
Lactic acid	1.33(d), 4.11(q)	0.981	−0.735
Alanine	1.47(d)	0.910	−0.753
Glycoprotein	2.03(s)	0.889	−0.828
Tyrosine	6.89(d), 7.18(d)	0.724	−0.810
Phenylalanine	7.32(m), 7.42(m)	0.894	−0.713
Pyruvic acid	2.37(s)	0.824	−0.802
Methionine	2.13(s)	0.930	−0.763
Creatine	3.03(s), 3.93(s)	0.866	−0.804
Citric acid	2.54(d), 2.68(d)	0.758	−0.721
Valine	0.99(d),1.05(d)	0.898	−0.759
Glutamic acid	2.07(m), 2.36(m), 3.75(m)	0.889	−0.830
Glutamine	2.16(m), 3.78(m)	0.884	−0.762
L (-)-Glutathione	3.27(m)	0.990	−0.654
Aspartic acid	2.67(dd), 2.82(dd)	0.859	−0.721
Glycerophosphorylcholine	3.22(s), 3.63(m)	0.843	−0.876
Ethanolamine phosphate	3.23(t), 3.99(m)	0.823	−0.833
Betaine	3.27(s), 3.90(s)	0.991	−0.655
Hypoxanthine	8.20(s), 8.22(s)	0.630	−0.817

Table 2
Important pathways in participation of differential metabolites DBJJ-HG *vs* model group.

Pathways	Raw p	FDR	Impact	Hits/Total
Phenylalanine, tyrosine and tryptophan biosynthesis	0.000 888 24	0.010 7	1	2/4
Alanine, aspartate and glutamate metabolism	0.000 000 534	2.24×10^{-5}	0.534	6/28
D-Glutamine and *D*-glutamate metabolism	0.002 187 4	0.020 4	0.5	2/6
Phenylalanine metabolism	0.009 199 5	0.070 2	0.357	2/12
Pyruvate metabolism	0.244 77	0.761 5	0.207	1/22
Tyrosine metabolism	0.095 954	0.447 8	0.14	2/42
Citrate cycle (TCA cycle)	0.024 941	0.139 7	0.137	2/20
Arginine biosynthesis	0.000 565 14	0.009 5	0.117	3/14
Cysteine and methionine metabolism	0.062 904	0.330 2	0.104	2/33
Glycolysis/ Gluconeogenesis	0.282 67	0.848 0	0.100	3/14

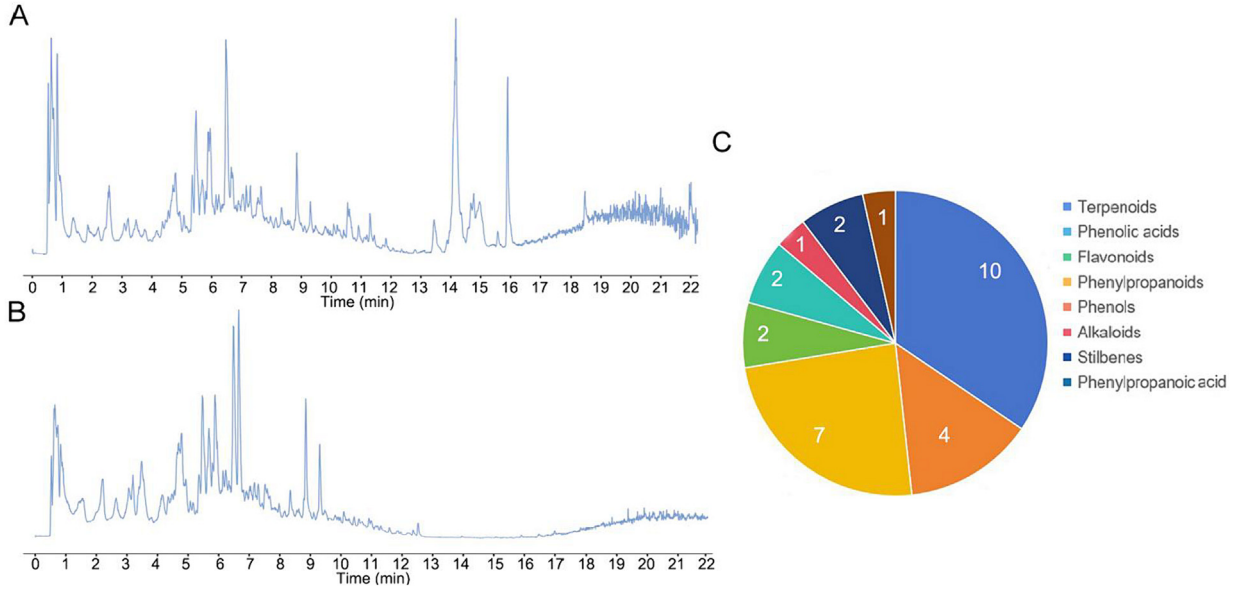

Fig. 5. Composition of DBJJ was determined by UPLC-QE-MS/MS.. Total ion chromatogram of DBJJ in positive (A) and negative (B) ion mode was obtained. Number of monomer components in DBJJ identified by UPLC-QE-MS/MS (C).

Table 3
Bioactive compounds of DBJJ.

Bioactive compounds	OB (%)	Caco-2	Molecular formula	PubChem CID	Class
Oleanic acid	29.02	0.59	$C_{30}H_{48}O_3$	10494	Terpenes
Chlorogenic acid	15.93	0.51	$C_{16}H_{18}O_9$	1794427	Phenolic acids
Caffeic acid	54.97	0.31	$C_9H_8O_4$	689043	Phenolic acids
Rutinum	74.29	0.93	$C_{27}H_30O_{16}$	5280805	Flavonoids
Ferulic acid	65.71	0.58	$C_{10}H_{10}O_4$	445858	Phenylalanine acid
Rosmarinic acid	70	0.93	$C_{18}H_{16}O_8$	5281792	Phenolic acids
Quercetin	49.07	0.64	$C_{15}H_{10}O_7$	5280343	Flavonoids
6-Methyl-1,4-oxazocane-5,8-dione	80	0.49	$C_7H_{11}NO_3$	162691670	Amides alkaloids
Ursolic acid	51.43	0.61	$C_{30}H_{48}O_3$	64945	Terpenes
Angustanoic acid F	55.71	0.8	$C_{20}H_{28}O_3$	10591519	Terpenes
1-Phenanthrenecarboxylic acid	72.86	0.86	$C_{15}H_{10}O_2$	284068	Terpenes
Angustanoic acid G	55.71	0.69	$C_{19}H_{24}O_3$	10709361	Phenolic acids
Jiadifenoic acid K	58.57	0.75	$C_{40}H_{52}O_5$	71525029	Diterpenes

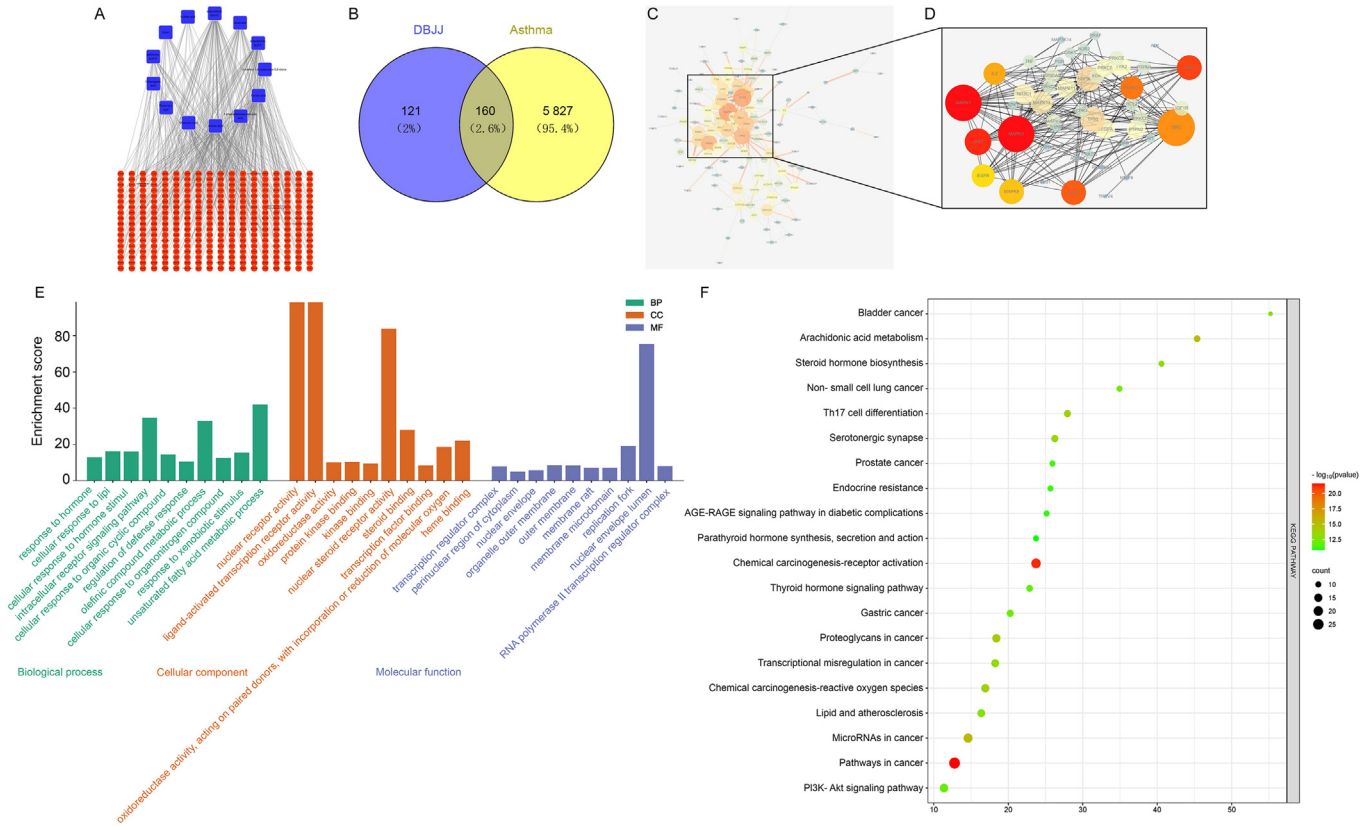

Fig. 6. DBJJ anti-asthma core target network pharmacological analysis. (A) Herb-active component–target interaction network of DBJJ. (The gene targets are described as red circles. Blue squares represent active component of DBJJ. Lines stand for relation of compounds and target nodes); (B) Active ingredient target-disease target intersection map (Blue and yellow areas show number of potential targets of DBJJ and asthma. The intersections indicate number of DBJJ-asthma common targets.); (C) PPI network of DBJJ in treatment of asthma (The degree of targets in submodules is indicated by color shade of node); (D) The hub targets of DBJJ in treatment of asthma (The degree of targets in the submodules is indicated by color shade of node); (E) GO enrichment analysis of core targets; (F) Top 20 KEGG pathways of core targets. The bubble size represents target number enrich in each entry, and the color represents the enrichment significance based on corrected *P* value.

3.10. Western blotting

To investigate the effects of DBJJ on asthma-related genes, we analyzed the expression of MAPK, STAT3, and NOS2 in lung tissue using immunoblot analysis. These genes were identified as the hub genes most closely related to asthma through network pharmacology analysis of DBJJ. Additionally, we examined the expression of common genes obtained through joint metabolomics and network pharmacology analysis. Our results revealed that the expression of MAPK, STAT3, and NOS2 was significantly increased in the lung tissue of the asthma model rats ($P < 0.01$). However, treatment with DBJJ resulted in a significant reduction in their expression and phosphorylation levels compared to the model group, and this difference was statistically significant (Fig. 8).

4. Discussion

4.1. Effects of DBJJ on asthma rats

Asthma is a complex disease with mechanisms that are not fully understood. Airway inflammation and airway remodeling are recognized as significant pathological features of asthma, and oxidative stress is also implicated in the development of airway

Table 4
Molecular docking score of DBJJ active components and key targets.

Compounds	Targets	Scores
Ferulic acid	DAO	−6.5
	MAMO	−6.6
	MAMB	−6.6
	NOS2	−8.1
1-Phenanthrenecarboxylic acid	DAO	−8.0
	MAMO	−7.9
	MAMB	−7.3
	NOS2	−9.9
6-Methyl-1,4-oxazocane-5,8-dione	DAO	−5.4
	MAMO	−5.8
	MAMB	−5.9
	NOS2	−6.4
Ursolic acid	DAO	−8.7
	MAMO	−8.1
	MAMB	−9.4
	NOS2	−9.4

remodeling (Michaeloudes et al., 2022). Inflammatory factors such as TNF-α, IL-18, Ig-E, EOS, and IL-1β are associated with asthma and play crucial roles in its pathogenesis. TNF-α and IL-1β are pro-inflammatory cytokines that can induce inflammation in airway epithelial cells and immune cells, resulting in airway constriction and increased mucus production (Contoli et al., 2006). IL-18 is known to activate immune cells such as Th1 and Th2, thereby promoting the initiation and persistence of inflammatory reactions (Nakanishi, Yoshimoto, Tsutsui, & Okamura, 2001). Ig-E, an immunoglobulin, plays a role in mediating allergic reactions and interacts with EOS cells (Gould & Sutton, 2008). EOS cells, as immune cells, can release inflammatory mediators like histamine, which can contribute to airway constriction and increased mucus production. These processes collectively contribute to the characteristic symptoms of asthma. VEGF-A and TGF-β1 are two growth factors related to airway remodeling, which can promote structural changes such as proliferation of airway smooth muscle cells and hyperplasia of mucous glands, leading to airway narrowing and asthma attacks (Liu et al., 2016). MDA and SOD are oxidative stress indicators related to asthma. MDA is a product of lipid peroxidation that reflects the extent of oxidative damage to cell membranes, while SOD is an antioxidant enzyme that helps remove superoxide anion free radicals in cells, thereby reducing oxidative stress damage. During asthma attacks, the level of oxidative stress increases, resulting in enhanced lipid peroxidation of cell membranes and decreased activity of intracellular antioxidant enzymes. This reduction in antioxidant capacity impairs the ability to clear free radicals effectively. All of these factors can lead to aggravated airway inflammation, airway smooth muscle contraction, and increase mucus secretion, ultimately resulting in the appearance of asthma symptoms (Comhair & Erzurum, 2010; Rahman, Biswas, & Kode, 2006). In this study, we treated asthmatic rats with DBJJ decoction and evaluated multiple indicators. We observed pathological morphological changes in the lung tissues of rats in each group using HE staining. DBJJ decoction significantly decreased the concentration of inflammatory factors, including TNF-α, IL-18, IgE, EOS, IL-1β, VEGF-A, and TGF-β1, in the serum of asthmatic rats. Furthermore, it increased the concentration of malondialdehyde (MDA), an oxidative stress marker. These findings suggest that DBJJ decoction may have a therapeutic effect on asthma by alleviating asthma symptoms and airway inflammation through multiple pathways.

4.2. ^{1}H NMR serum metabolomics

The analysis of terminal metabolites in organisms through metabolomics has the capability to detect even the slightest alterations in biological pathways, thereby facilitating a comprehensive comprehension of the efficacy mechanism of traditional Chinese medicine (Cai et al., 2019; Ding et al., 2018). In this study, the serum metabolites of rats were examined using the ^{1}H NMR tech-

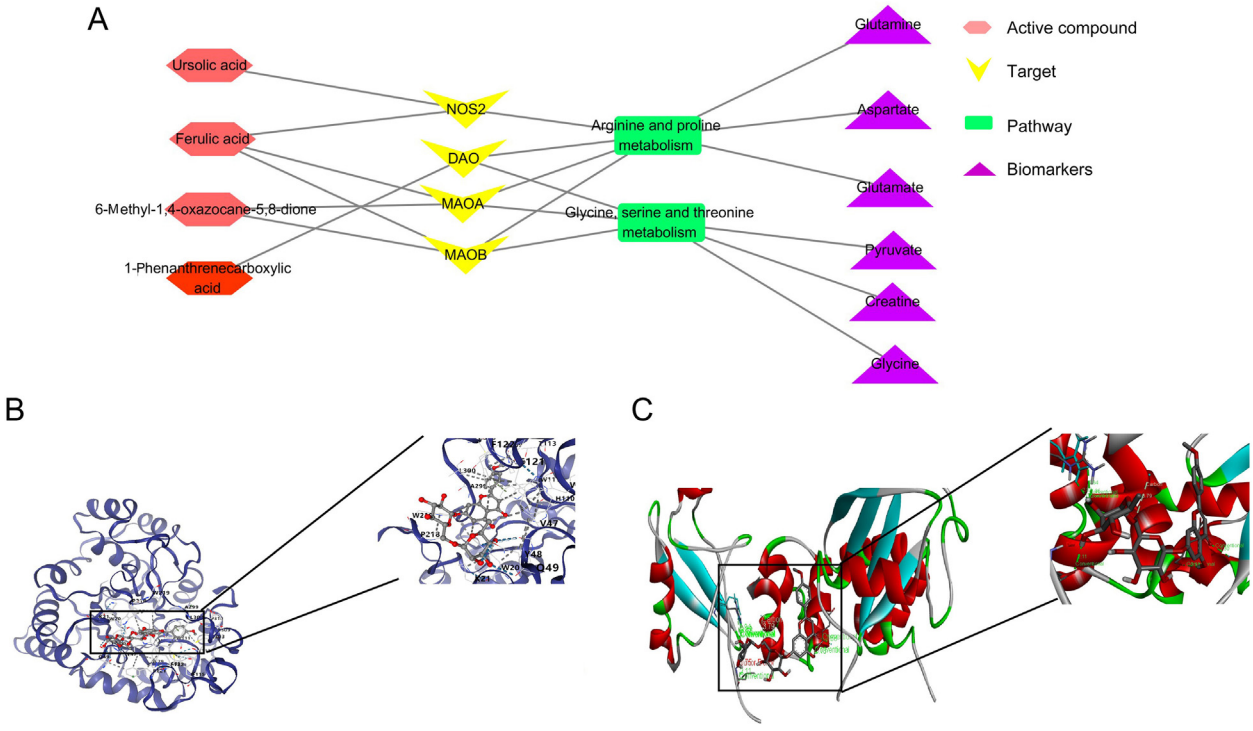

Fig. 7. (A) Active compound-target-pathway-biomarkers interaction network of DBJJ treating asthma. (B) Docking between ferulic acid and DAO. (C) Docking between 1-phenanthrenecarboxylic acid and NOS2.

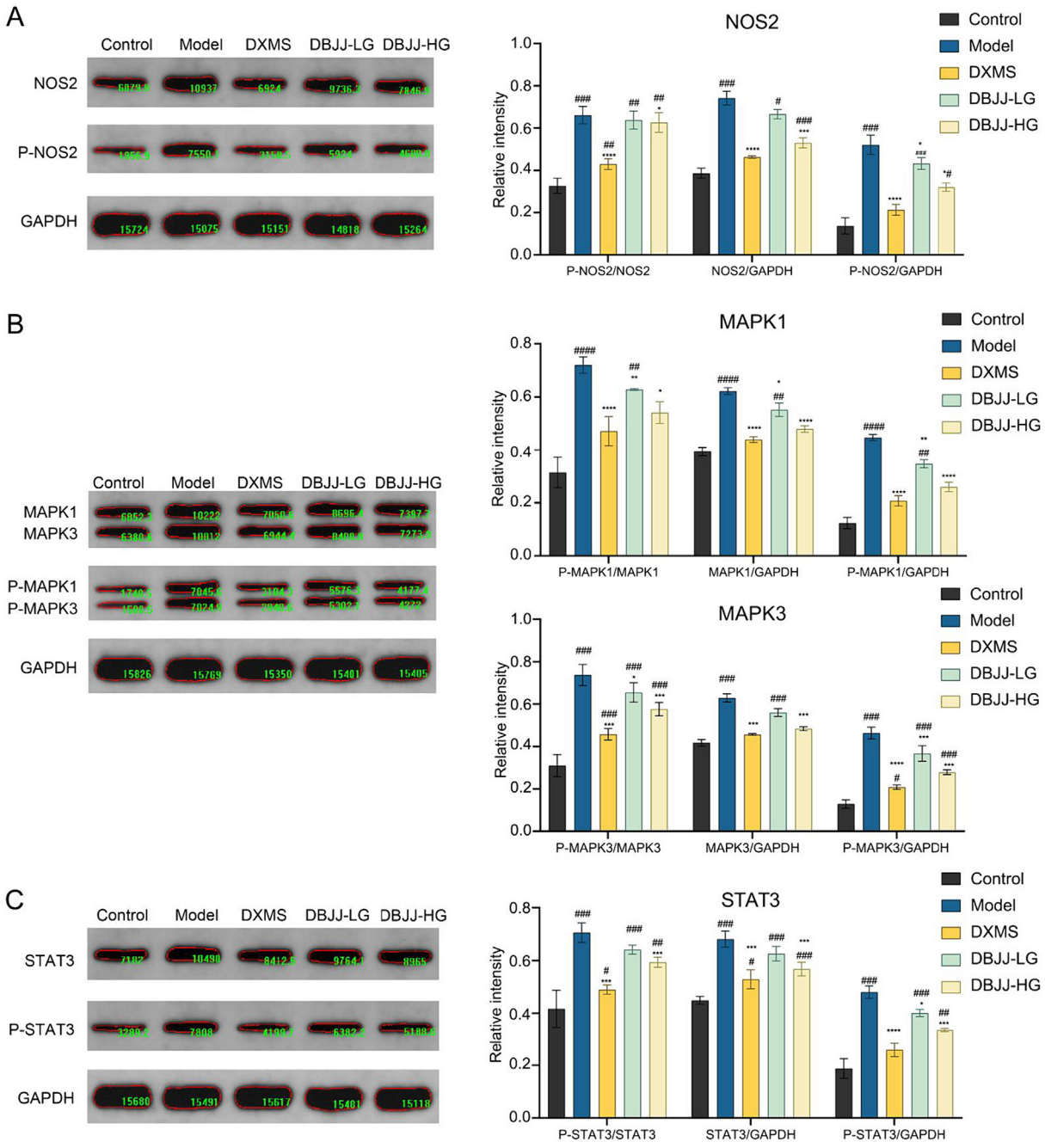

Fig. 8. Effects of DBJJ on altered phosphorylation levels and expression of NOS2, P-NOS2, MAPK1, MAPK3, P-MAPK1, P-MAPK3, STAT3 and P-STAT3 proteins in the lung tissue of asthmatic rats.

nique, leading to the establishment of the serum metabolic fingerprints of asthmatic rats. Furthermore, differential endogenous metabolites were identified through the utilization of PCA, PLS-DA, and OPLS-DA analyses. The findings indicate that the metabolic profile among groups differed significantly, as evidenced by the spatial scatter diagram of PLS-DA analysis. The findings of our study demonstrate significant differences in the metabolic profiles among the groups, as indicated by the spatial scatter diagram obtained from the PLS-DA analysis. Notably, the DBJJ group exhibited a closer proximity to the blank group, suggesting that DBJJ may have a relieving effect on asthma. Further analysis revealed that DBJJ had a significant impact on 20 metabolites in the serum of asthmatic rats, including phenylalanine, glutamic acid, and glycine. The findings indicate that DBJJ may modulate the levels of these metabolites, thereby influencing amino acid metabolism, protein metabolism, and energy metabolism in asthmatic rats. Hence, DBJJ has the potential to modulate the metabolic pathways and alter the physiological state of asthmatic rats, thereby mitigating the symptoms of asthma. These findings offer a significant insight into the pharmacodynamic mechanism of DBJJ and facilitate the exploration of its therapeutic mechanism for asthma.

4.3. UPLC-QE-MS/MS combined with network pharmacology analysis

The integration of UPLC-QE-MS/MS technology and network pharmacological analysis presents several advantages. UPLC-QE-MS/MS technology enables swift and effective separation and identification of components in traditional Chinese medicine (Miao

et al., 2023). The amalgamation of these two techniques enables a comprehensive assessment of the effects of multiple compounds and their interactions with targets, thereby aiding in the elucidation of the intricate mechanisms involved (Lu, Qiu, Fan, Yu, & Wu, 2021; Wang et al., 2022). In this study, UPLC-QE-MS/MS technology identified 29 compounds, and specific criteria were applied to screen the active ingredients of DBJJ. The component-target-disease network analysis revealed that 120 target genes were closely associated with the 13 active components of DBJJ, and that 173 pathways could be regulated to improve asthma. KEGG database analysis further demonstrated that target genes such as Th17 cell differentiation and the PI3K-Akt signaling pathway.

DBJJ's anti-asthma effect may be attributed to four primary components, namely ferulic acid and ursolic acid, which act upon four targets including DAO, MAOA, MAOB, and NOS2. These components and targets are involved in the metabolic pathway of glycine, serine, and threonine and have an impact on six crucial metabolites such as glutamic acid and glycine. The findings suggest that DBJJ exerts its anti-asthma effect through various components, targets, and metabolic pathways, thereby influencing multiple crucial metabolites. This underscores the significance of the synergistic effects of multiple components and targets in traditional Chinese medicine formulations, as opposed to the action of a solitary component or target. These results offer a valuable lead for further exploration into the anti-asthma mechanism of DBJJ and provide a theoretical foundation for its development and application.

Molecular docking represents a valuable tool for comprehending the action mechanisms of drugs and can assist in advancing our understanding of their modes of action (Liu, Mao, Gu, He, & Hu, 2021; Pinzi & Rastelli, 2019).Our results demonstrate that ferulic acid and ursolic acid, the active components of DBJJ, bind to the core targets of DAO and NOS2 through ionic, hydrogen, and π-π bonds, suggesting a strong interaction between them. These findings provide important clues for further investigation into the anti-asthma mechanism of DBJJ and offer a theoretical basis for its development and application.

4.4. Hub target protein expression

The present study utilized Western blotting to investigate the expression of critical genes linked to asthma, specifically MAPK1, MAPK3, and STAT3, which were identified as hub genes through DBJJ network pharmacology, in addition to the common gene NOS2, which was identified through a combined analysis of metabolomics and network pharmacology. The results of our investigation demonstrated that treatment with DBJJ led to a decrease in both the expression and phosphorylation levels of MAPK1, MAPK3, NOS2, STAT3 in asthma rat's lung tissue. MAPK1 and MAPK3 are two types of mitogen-activated protein kinases (MAPKs) involved in various cellular signal transduction pathways, including those related to asthma-induced inflammatory response (Alam & Gorska, 2011; Duan, Chan, Wong, Leung, & Wong, 2004). During the pathophysiological process of asthma, inflammatory mediators such as cytokines and chemical mediators can stimulate the phosphorylation of MAPK1 and MAPK3, thereby promoting airway inflammation and muscle contraction, leading to the onset and exacerbation of asthma symptoms (Bhavsar, Khorasani, Hew, Johnson, & Chung, 2010; Zhu, Xiao, Dong, & Yuan, 2023). Therefore, reducing the expression and phosphorylation levels of MAPK1 and MAPK3 may help to curb the inflammatory response and alleviate asthma symptoms. NOS2 is an inducible nitric oxide synthase that plays a pivotal role in the pathophysiology of asthma (Chunxian DU, Xu, & Ye, 2002; Filipczak et al., 2003). During an asthma attack, inflammatory cells and epithelial cells can stimulate the expression and activity of NOS2, leading to the production of large amounts of nitric oxide. Nitric oxide can not only promote airway smooth muscle contraction and mucus secretion, but also increase airway permeability and inflammatory cell infiltration, resulting in the aggravation of asthma symptoms (Eriksson et al., 2005). Hence, reducing the expression and activity of NOS2 may aid in alleviating asthma symptoms and controlling asthma attacks. STAT3 is a signal transducer and transcriptional activator that participates in various cellular biological processes, including inflammatory responses (He et al., 2018; Lim, Cho, Choi, Na, & Chung, 2015). In the pathophysiological process of asthma, inflammatory cells and epithelial cells can stimulate the expression and activity of STAT3, thus promoting airway inflammation and muscle contraction, leading to the onset and exacerbation of asthma symptoms (Kharitonov & Barnes, 2003). Additionally, STAT3 can regulate the immune response of T cells and B cells, thus affecting asthma development (Wang, Shen, Wang, Shen, & Zhou, 2018). Therefore, reducing the expression and activity of STAT3 may help to suppress the inflammatory response and alleviate asthma symptoms.

5. Conclusion

The administration of DBJJ demonstrates notable anti-asthma properties in rats with allergic asthma. It is achieved through the effect of the primary constituents such as ferulic acid and ursolic acid of DBJJ on targets such as NOS2, MAPK, and STAT3, thereby influencing arginine and proline metabolism as well as glycine, serine, and threonine metabolism. These results serve as a solid foundation for further discussions and research on the anti-asthma properties of DBJJ. The study establishes a basis for future exploration of the anti-asthmatic properties of DBJJ and its potential utilization in clinical settings.

CRediT authorship contribution statement

Kailibinuer Abulaiti: Data curation, Formal analysis, Visualization, Writing – original draft. **Miheleayi Aikepa:** Formal analysis, Visualization. **Mireguli Ainaidu:** Formal analysis, Data curation. **Jiaxin Wang:** Writing – original draft. **Maiwulanijiang Yizibula:** Formal analysis, Visualization. **Maihesumu Aikemu:** Validation, Writing – review & editing, Project administration.

Declaration of Competing Interest

The authors declare that they have no known competing financial interests or personal relationships that could have appeared to influence the work reported in this paper.

Acknowledgments

This work was financially supported by Xinjiang Uygur Autonomous Region Department of Science and Technology (No. 2016A03005-1).

Appendix A. Supplementary material

Supplementary data to this article can be found online at https://doi.org/10.1016/j.chmed.2024.02.001.

References

2 GINA Report, Global Strategy for Asthma Management and Prevention. https://ginasthma.org/gina-reports/.

Alam, R., & Gorska, M. (2011). Mitogen-activated protein kinase signalling and ERK1/2 bistability in asthma. *Clinical and Experimental Allergy: Journal of the British Society for Allergy and Clinical Immunology, 41*(2), 149–159.

Bhavsar, P., Khorasani, N., Hew, M., Johnson, M., & Chung, K. F. (2010). Effect of p38 MAPK inhibition on corticosteroid suppression of cytokine release in severe asthma. *European Respiratory Journal, 35*(4), 750–756.

Borna, E., Nwaru, B., Bjerg, A., Mincheva, R., Rådinger, M., Lundbäck, B., & Ekerljung, L. (2019). Changes in the prevalence of asthma and respiratory symptoms in western Sweden between 2008 and 2016. *Allergy: European Journal of Allergy and Clinical Immunology, 74*(9), 1703–1715.

Cai, Y., Zhao, M., Guan, Z., Han, X., Wang, M., & Zhao, C. (2019). Metabolomics analysis of the therapeutic mechanism of *Semen Descurainiae* Oil on hyperlipidemia rats using ^{1}H-NMR and LC-MS. *Biomedical Chromatography, 33*(10), e4536.

Cevhertas, L., Ogulur, I., Maurer, D., Burla, D., Ding, M., Jansen, K., & Akdis, C. (2020). Advances and recent developments in asthma in 2020. *Allergy: European Journal of Allergy and Clinical Immunology, 75*(12), 3124–3146.

Charles, D., Shanley, J., Temple, S. N., Rattu, A., Khaleva, E., & Roberts, G. (2022). Real-world efficacy of treatment with benralizumab, dupilumab, mepolizumab and reslizumab for severe asthma: A systematic review and meta-analysis. *Clinical and Experimental Allergy, 52*(5), 616–627.

Chunxian, D., Xu, Q., & Ye, Y. (2002). Expression of Fas and NOS-2 in airway epithelial cells of asthma guinea pigs. *Medical Journal of Wuhan University, 23*(2), 114–117.

Cloutier, M. M., Dixon, A. E., Krishnan, J. A., Lemanske, R. F., Jr., Pace, W., & Schatz, M. (2020). Managing asthma in adolescents and adults: 2020 Asthma guideline update from the national asthma education and prevention program. *Journal of the American Medical Association, 324*(22), 2301–2317.

Comhair, S. A., & Erzurum, S. C. (2010). Redox control of asthma: Molecular mechanisms and therapeutic opportunities. *Antioxidants & Redox Signaling, 12*(1), 93–124.

Contoli, M., Message, S. D., Laza-Stanca, V., Edwards, M. R., Wark, P. A., Bartlett, N. W., & Johnston, S. L. (2006). Role of deficient type III interferon-lambda production in asthma exacerbations. *Nature Medicine, 12*(9), 1023–1026.

Ding, M., Li, Z., Yu, X. A., Zhang, D., Li, J., Wang, H., & Chang, Y. X. (2018). A network pharmacology-integrated metabolomics strategy for clarifying the difference between effective compounds of raw and processed Farfarae flos by ultra high-performance liquid chromatography-quadrupole-time of flight mass spectrometry. *Journal of Pharmaceutical and Biomedical Analysis, 156*, 349–357.

Dolkun, P., Abduwak, M., Jinfang, Z., Ye, L., & Anwar, M. (2022). Individual determination of two kinds of flavonoids and their glycosides in *Nepeta bracteat*a by HPLC. *Science and Technology of Food Industry, 43*(15), 289–297.

Duan, W., Chan, J. H., Wong, C. H., Leung, B. P., & Wong, W. S. (2004). Anti-inflammatory effects of mitogen-activated protein kinase kinase inhibitor U0126 in an asthma mouse model. *Journal of Immunology, 172*(11), 7053–7059.

Ducharme, F. M., Tse, S. M., & Chauhan, B. (2014). Diagnosis, management, and prognosis of preschool wheeze. *The Lancet, 383*(9928), 1593–1604.

Eriksson, U., Egermann, U., Bihl, M. P., Gambazzi, F., Tamm, M., Holt, P. G., & Bingisser, R. M. (2005). Human bronchial epithelium controls TH2 responses by TH1-induced, nitric oxide-mediated STAT5 dephosphorylation: Implications for the pathogenesis of asthma. *Journal of Immunology, 175*(4), 2715–2720.

Filipczak, P. T., Senft, A. P., Seagrave, J., Weber, W., Kuehl, P. J., Fredenburgh, L. E., McDonald, J. D., & Baron, R, M. (2015). NOS-2 inhibition in phosgene-induced acute lung injury. *Toxicological Sciences, 146*(1), 89–100.

Gould, H. J., & Sutton, B. J. (2008). IgE in allergy and asthma today. *Nature Reviews Immunology, 8*(3), 205–217.

He, Y., Lou, X., Jin, Z., Yu, L., Deng, L., & Wan, H. (2018). Mahuang decoction mitigates airway inflammation and regulates IL-21/STAT3 signaling pathway in rat asthma model. *Journal of Ethnopharmacology, 224*, 373–380.

Kharitonov, S. A., & Barnes, P. J. (2003). Nitric oxide, nitrotyrosine, and nitric oxide modulators in asthma and chronic obstructive pulmonary disease. *Current Allergy and Asthma Reports, 3*(2), 121–129.

Kianmeher, M., Ghorani, V., & Boskabady, M. H. (2016). Animal model of asthma, various methods and measured parameters: A methodological review. *Iranian Journal of Allergy, Asthma, and Immunology, 15*(6), 445–465.

Lim, H., Cho, M., Choi, G., Na, H., & Chung, Y. (2015). Dynamic control of Th2 cell responses by STAT3 during allergic lung inflammation in mice. *International Immunopharmacology, 28*(2), 846–853.

Liu, R., Mao, Y., Gu, Z., He, J., & Hu, C. (2021). Network pharmacology-based analysis of the underlying mechanism of *Hyssopus cuspidatus* Boriss. for antiasthma: A characteristic medicinal material in Xinjiang. *Evidence-based Complementary and Alternative Medicine, 2021*, 1–13.

Liu, Y., Li, Y., Li, N., Teng, W., Wang, M., Zhang, Y., & Xiao, Z. (2016). TGF-β1 promotes scar fibroblasts proliferation and transdifferentiation via up-regulating MicroRNA-21. *Scientific Reports, 6*, 32231.

Lu, W. W., Qiu, Y. J., Fan, X. F., Yu, G. Y., & Wu, G. L. (2021). Mechanism of Huangqi Guizhi Wuwu decoction in treatment of rheumatoid arthritis based on UPLC-LTQ-Orbitrap-MS, network pharmacology, and cell experiment. *China Journal of Chinese Materia Medica, 46*(24), 6454–6464.

Maleki, S. J., Crespo, J. F., & Cabanillas, B. (2019). Anti-inflammatory effects of flavonoids. *Food Chemistry, 299*, 125124.

Miao, Y., Fan, X., Wei, L., Wang, B., Diao, F., Fu, J., & Zhang, Y. (2023). Lizhong decoction ameliorates pulmonary infection secondary to severe traumatic brain injury in rats by regulating the intestinal physical barrier and immune response. *Journal of Ethnopharmacology, 311*, 116346.

Nakanishi, K., Yoshimoto, T., Tsutsui, H., & Okamura, H. (2001). Interleukin-18 is a unique cytokine that stimulates both Th1 and Th2 responses depending on its cytokine milieu. *Cytokine & Growth Factor Reviews, 12*(1), 53–72.

Niu, W., Miao, J., Li, X., Guo, Q., Deng, Z., & Wu, L. (2022). Metabolomics combined with systematic pharmacology reveals the therapeutic effects of *Salvia miltiorrhiza* and *Radix Pueraria lobata* herb pair on type 2 diabetes rats. *Journal of Functional Foods, 89*, 104950.

Pinzi, L., & Rastelli, G. (2019). Molecular docking: Shifting paradigms in drug discovery. *International Journal of Molecular Sciences, 20*(18), 4331.

Rahman, I., Biswas, S. K., & Kode, A. (2006). Oxidant and antioxidant balance in the airways and airway diseases. *European Journal of Pharmacology, 533*(1–3), 222–239.

Sun, H., Zhang, H. L., Zhang, A. H., Zhou, X. H., Wang, X. Q., Han, Y., ... Wang, X. J. (2018). Network pharmacology combined with functional metabolomics discover bile acid metabolism as a promising target for mirabilite against colorectal cancer. *RSC Advances, 8*(53), 30061–30070.

Wang, J., Li, F. S., Pang, N. N., Tian, G., Jiang, M., Zhang, H. P., & Ding, J. B. (2016). Inhibition of asthma in OVA sensitized mice model by a traditional Uygur herb *Nepeta bracteata* Benth. *Evidence-Based Complementary and Alternative Medicine, 2016*, 5769897.

Wang, L., Du, Z., Guan, Y., Wang, B., Pei, Y., Zhang, L., & Fang, M. (2022). Identifying absorbable bioactive constituents of Yupingfeng Powder acting on COVID-19 through integration of UPLC-Q/TOF-MS and network pharmacology analysis. *Chinese Herbal Medicines, 14*(2), 283–293.

Wang, Y., Shen, Y., Wang, S., Shen, Q., & Zhou, X. (2018). The role of STAT3 in leading the crosstalk between human cancers and the immune system. *Cancer Letters, 415*, 117–128.

Wu, T. D., Brigham, E. P., & McCormack, M. C. (2019). Asthma in the primary care setting. *Medical Clinics of North America, 103*(3), 435–452.

Yang, E. L., Hou, Y., Ma, G. X., Zou, L. J., Xu, X. D., Wu, H. F., & Shi, L. L. (2022). Abietane-type diterpenoids from *Nepeta bracteata* Benth. and their anti-inflammatory activity. *Frontiers Chemistry, 10*, 944972.

Yusupu, A., & Aikemu, M. (2016). The preparation method and applications of a total flavonoid extract from Nepeta bracteata Benth. [Patent No. CN201610914262.8]. China.

Zhang, G. J., Miao, J., Guo, L. Y., Jia, J. W., & Cui, H. T. (2021). Application of multi-omics combination in mechanism studies of traditional Chinese medicine. *Chinese Traditional and Herbal Drugs, 52*(10), 3112–3120.

Zhang, M., Chen, M., Hou, Y., Fan, C., Wei, H., Shi, L., & Zhang, J. (2021). Inflammatory and cytotoxic activities of abietane terpenoids from *Nepeta bracteata* Benth. *Immunological Journal, 26*(18), 5603.

Zhang, Z., Yi, P., et al. (2020). Integrated network pharmacology analysis and serum metabolomics to reveal the cognitive improvement effect of Bushen Tiansui formula on Alzheimer's disease. *Journal of Ethnopharmacology, 249*, 112371.

Zhu, T., Xiao, X., Dong, Y., & Yuan, C. (2023). Neferine alleviates ovalbumin-induced asthma via MAPK signaling pathways in mice. *Allergologia et Immunopathologia, 51*(3), 135–142.